CHANNELS
2016, VOL. 10, NO. 4, 320–331
http://dx.doi.org/10.1080/19336950.2016.1168551

Taylor & Francis
Taylor & Francis Group

ARTICLE ADDENDUM

Fine-tuning of eTRPM8 expression and activity conditions keratinocyte fate

Gabriel Bidaux[a,b,c], Anne-Sophie Borowiec[a], Natalia Prevarskaya[a], and Dmitri Gordienko[a,d]

[a]Inserm U-1003, Equipe labellisée par la Ligue Nationale contre le cancer, Université des Sciences et Technologies de Lille (USTL), Villeneuve d'Ascq, Bron, France; [b]Univ Lyon, CarMeN laboratory, Inserm UMR1060, INRA UMR1397, Insa-Lyon, Bron, France; [c]IHU OPERA, Hospices Civils de Lyon, Groupement Hospitalier EST, Bron, France; [d]Laboratory of Molecular Pharmacology and Biophysics of Cell Signaling; Bogomoletz Institute of Physiology, Kiev, Ukraine

ABSTRACT

Recently, we reported the cloning and characterization of short isoform of the icilin-activated cold receptor TRPM8 channel in keratinocytes, dubbed eTRPM8. We demonstrated that eTRPM8 via fine tuning of the endoplasmic reticulum (ER) – mitochondria Ca^{2+} shuttling regulates mitochondrial ATP and superoxide ($O_2^{\bullet-}$) production and, thereby, mediates control of epidermal homeostasis by mild cold. Here, we provide additional information explaining why eTRPM8 suppression and TRPM8 stimulation both inhibit keratinocyte growth. We also demonstrate that stimulation of eTRPM8 with icilin may give rise to sustained oscillatory responses. Furthermore, we show that ATP-induced cytosolic and mitochondrial Ca^{2+} responses are attenuated by eTRPM8 suppression. This suggests positive interplay between eTRPM8 and purinergic signaling pathways, what may serve to facilitate the ER-mitochondria Ca^{2+} shuttling. Finally, we demonstrate that cold (25°C) induces eTRPM8-dependent superoxide-mediated necrosis of keratinocytes. Altogether, these results are in line with our model of eTRPM8-mediated cold-dependent balance between keratinocyte proliferation and differentiation.

ARTICLE HISTORY
Received 22 February 2016
Revised 9 March 2016
Accepted 14 March 2016

KEYWORDS
ATP; bioenergetics; cell death; cell physiology; differentiation; epidermal homeostasis; ER Calcium fluxes; eTRPM8; mild cold; mitochondria; proliferation; ROS; superoxide; TRPM8 channels

Introduction

Under influence of ambient factors, the skin epidermis undergoes continuous regeneration through so-called epidermal homeostasis (EH): the fine-tuning of the balance between proliferation, directional migration, differentiation and death of keratinocytes. Deviation of the ambient temperature is one of the most important stimuli which constantly affect mammals' skin. Changes in the ambient temperature are perceived by thermoreceptors, the ion channels which belong to the transient receptor potential (TRP) super family (for a review see ref.[1]). Keratinocytes may directly transduce thermal stimuli via warmth-activated TRP channels, TRPV3 (with an apparent threshold of about 32–39°C) and TRPV4 (27–34°C).[2-4] Nevertheless, it is important to note that at ambient temperatures from +10°C to +30°C, the unprotected human skin temperature settles at mean steady-state values within the range of +24°C to +33°C, respectively,[5] which is within the functional range of TRPM8 cold sensitivity.[6,7] Yet, the molecular identification of the cold transducer which translates cooling into downstream signaling events in keratinocytes was lacking.

In a recent investigation,[8] we reported the cloning and characterization of a new 4-trasmembrane-domain epidermal isoform of the TRPM8 cold receptor-channel, dubbed eTRPM8. This channel is localized and functions in the keratinocyte endoplasmic reticulum (ER) membrane but not in the plasmalemma. Activation of eTRPM8 within ER-mitochondria contact sites facilitates mitochondrial Ca^{2+} uptake, thus, affecting mitochondrial Ca^{2+} concentration ($[Ca^{2+}]_m$). In turn, $[Ca^{2+}]_m$ modulates ATP and superoxide ($O_2^{\bullet-}$) synthesis. We reported that this fine-tuning of ATP and $O_2^{\bullet-}$ levels by cooling temperatures controls the balance between proliferation and differentiation of keratinocytes. Finally, by means of functional TRPM8 KO mouse line, we demonstrated that eTRPM8 suppression impairs the epidermis adaptation to low temperatures and general skin

CONTACT Gabriel Bidaux gabriel.bidaux@univ-lyon1.fr IHU OPERA Bron, Groupement Hospitalier EST, 69500 Bron, France.

Color versions of one or more of the figures in the article can be found online at www.tandfonline.com/kchl

Addendum to: Bidaux G, et al. Epidermal TRPM8 channel isoform controls the balance between keratinocyte proliferation and differentiation in a cold-dependent manner. Proc Natl Acad Sci U S A. 2015 Jun 30; 112(26):E3345-54; http://dx.doi.org/10.1073/pnas.1423357112

homeostasis. Based on this observations, we proposed a model according to which eTRPM8 regulates epidermal homeostasis in a cold-dependent manner. Yet, as in majority of studies conducted on "molecule-to-organism" scale, we utilized certain extrapolations, e.g., relation of $[Ca^{2+}]_m$ responses to acute stimulation (recorded on a time scale of seconds) to the steady-state $[Ca^{2+}]_m$ (monitored on a time scale of days). Also, due to space limitations, some interesting observations were bypassed in our recent publication.[8]

Here we provide these results to reinforce our hypothesis with additional insights. Firstly, we demonstrate that the modalities of eTRPM8 activation define the cell response toward proliferation or differentiation. While sustained stimuli slowed down cell cycle and induced differentiation, repeated transient stimuli increased proliferation rate. Secondly, we provide additional evidence for positive interplay between eTRPM8 and purinergic signaling pathways, which may serve to facilitate the ER-mitochondria Ca^{2+} shuttling. Namely, we demonstrate that ATP-induced Ca^{2+} release from the ER and concurrent mitochondrial Ca^{2+} uptake depend on eTRPM8 activity. Thirdly, we show that icilin, mimicking cold stimulation, induces an eTRPM8 oscillatory activity lasting at least for tens of minutes. Finally, we complement our previously reported observation, that the decrease of the ratio of proliferating to the late differentiated keratinocytes dropped after a 3-days incubation at 25°C is associated with an increase of $O_2^{\bullet-}$ content in an eTRPM8-dependent manner,[8,9] with demonstration that prolonged cold (25°C)-incubation decreases both $[Ca^{2+}]_m$and $[Ca^{2+}]_{ER}$ and facilitates ROS-mediated necrosis of keratinocytes.

This addendum along with our recent publication [8] demonstrate that both the eTRPM8 expression level and the modalities of cold-stimulation serve as important determinants of the keratinocyte fate and act via fine tuning of [ATP] and $[O_2^{\bullet-}]$.

Results and discussion

Either sustained stimulation of eTRPM8 or its knockdown, both decrease cell growth

In two recent studies,[8,9] we reported that cold incubation of keratinocytes impairs their growth. We also cloned and characterized a novel archetype of TRP channels in epidermis,[8] dubbed eTRPM8, and we demonstrated that it was a functional channel with 4 transmembrane domains (Fig. 1A) instead of the 6 original in full-length TRPM8. We also demonstrated that icilin application on the shaved skin of mice deceases the proliferation index of keratinocytes in an eTRPM8-dependent manner.[8] Fig. 1B shows that this effect can be reproduced by a 3-day incubation of HaCaT cell line in a medium supplemented with 20 μM icilin (renewed daily). Because Icilin is not very stable at 37°C, we have chosen a 20 μM concentration to prevent loss of effect due to degradation. eTRPM8 Knockdown prevented pulsed iciline-mediated increase in cell growth at 37°C (Fig. 1C) and thus demonstrate eTRPM8 specific effect of icilin. qPCR experiment revealed no modification in eTRPM8 expression level in HaCaT cells incubated at 31°C or in the presence of icilin (Fig. 1D). In contrast, incubation of the cells at 25°C enhanced eTRPM8 expression. This is in a line with the observation that the incubation at 25°C causes stronger reduction of the cell growth than incubation at 31°C or with icilin (Fig. 1B). Yet, the reduction of HaCaT cell growth caused by incubation with icilin or at 31°C was observed only in the cells expressing eTRPM8.

To what extent the modalities (i.e., intensity, duration and frequency) of eTRPM8 stimulation may affect the cell fate? To address this we explored the effect of "pulsed" stimulation HaCaT cells with icilin. In these experiments, the cells were exposed to icilin for 10 min per hour 8 times a day during 3 d. In contrast to sustained 3-day stimulation, which reduces the cell growth, the pulsed stimulation increases the cell growth about 1.4 times (Fig. 1B). This demonstrates that the modality of icilin stimulus can evoke the opposite effects on cell growth. This effect is eTRPM8 specific, since pulsed icilin stimulation did not augment the growth of eTRPM8-silenced HaCaT cells (Fig. 1C and E). Notably, sustained icilin stimulation reduces the cell growth to the same extent as eTRPM8 suppression (Fig. 1B and C). It was previously reported that over time, the activity of full-length TRPM8 run down in a PIP_2-dependent manner.[10] The eTRPM8 activity also strongly depends in bioavailability of PIP_2 [8] and, therefore, should be regulated in the same way. Also, enhanced Ca^{2+} leak from the ER caused by sustained stimulation of eTRPM8 may lead to the decrease of the ER calcium load (Fig. 3C and E). Both the ER depletion and eTRPM8 desensitization should, over time, reduce the ER-mitochondria Ca^{2+} transfer. It, therefore, seems likely that either suppression of eTRPM8 or its sustained activation by icilin may have similar effect on the cell

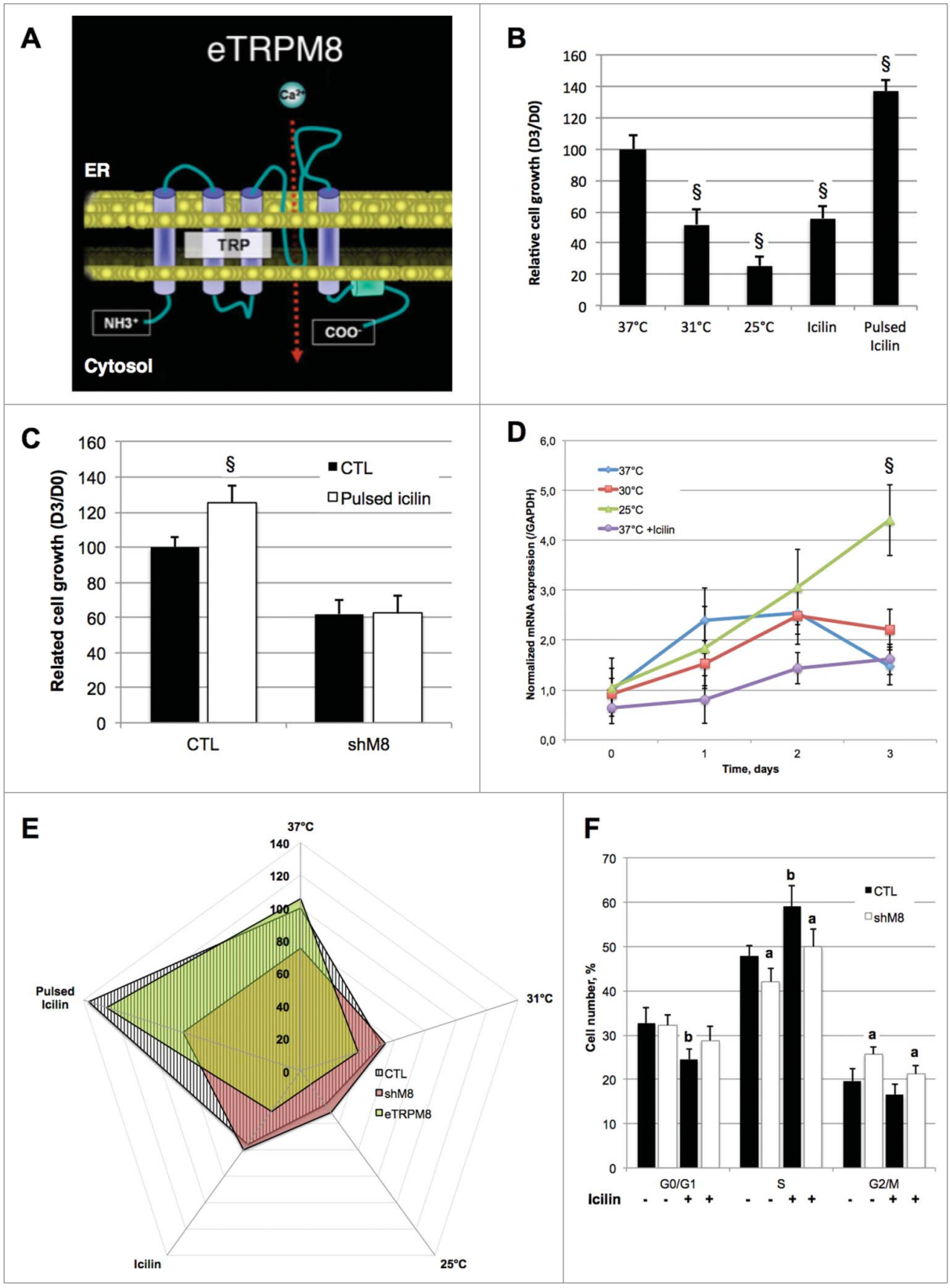

Figure 1. (For figure legend, see page 323.)

growth, even though they engage different mechanisms to control keratinocyte cell cycle. This hypothesis was supported by the results of FACS experiments (see in Methods). The proportion of the cells entering cell cycle decreased following sustained incubation with 20 μM iciline, while the population of the cells in S-phase increased (Fig. 1F). This suggests that icilin increases the number of proliferating cell while it slows down of cell cycle. Conversely to icilin treatment, the proportion of non-proliferating cells was similar between control cells and eTRPM8 KD cells, while the fraction of the cells in G2/M-phase was larger in eTRPM8 KD keratinocytes than control cells – suggesting a long-lasting arrest at G2/M checkpoint. In summary, this demonstrates that the suppression and sustained stimulation of eTRPM8 engage different signaling pathways, even though the end effect on the cell growth was similar.

A positive interplay between eTRPM8 and purinergic signaling pathways promotes keratinocytes proliferation

In Bidaux et al.,[8] we demonstrated correlation between thermo-dependent dynamics of [ATP] changes and the dynamics of the cell growth, but did not provide any evidence that eTRPM8-mediated proliferation of keratinocytes at 37°C may recruit ATP-linked signaling pathways. Activation of P2Y receptors (P2YRs) via $InsP_3$ production stimulates the ER-to-mitochondria Ca^{2+} shuttling via inositol trisphosphate receptors, $InsP_3Rs$.[11,12] We, therefore, assessed whether eTRPM8 activity affects in any way the $InsP_3R$-mediated Ca^{2+} shuttling facilitated by P2YR activation. We found that 30 μM suramin, the P2YR inhibitor, decreases the growth of control HaCaT cells by 2.2-fold, while it reduces the growth of eTRPM8 KD HaCaT cells only by 1.4-fold (Fig. 2A). Furthermore, using confocal imaging of fluo-4 and rhod-2 fluorescence, we compared ATP-induced changes in $[Ca^{2+}]_c$ and $[Ca^{2+}]_m$ in control HaCaT cells (Fig. 2B), in HaCaT cells pre-treated with the TRPM8 inhibitor capsazepine (Fig. 2C) and in eTRPM8 KD cells (Fig. 2D). Either eTRPM8 inhibition or suppression both augmented the ATP-induced $[Ca^{2+}]_c$ responses (Fig. 2E, panel a) and significantly attenuated concurrent mitochondrial Ca^{2+} uptake (Fig. 2E, panel b), as reported by the reduction of the $[Ca^{2+}]_m$ response. This demonstrates that, at 37°C, eTRPM8 is recruited to the ER-to-mitochondria Ca^{2+} shuttling process engaged by purinergic signaling pathways, and is in line with observed decrease of the cell proliferation (Fig. 1C). Furthermore, the effect of capsazepine indicates that the ER-to-mitochondria Ca^{2+} shuttling, engaged by purinergic stimulation, is regulated by the eTRPM8 channel activity rather than by interaction of the eTRPM8 protein with $InsP_3R$.

Activation of eTRPM8 induces long-lasting oscillatory Ca^{2+} shuttling from the ER to mitochondria and prevents the loss of Ca^{2+} in the mitochondrial matrix during hypothermia

We reported previously that cold or icilin-mediated activation of eTRPM8 induced Ca^{2+} shuttling from the ER to mitochondria on the time scale of seconds. It is not clear, however, whether a single robust Ca^{2+} uptake into mitochondria can maintain $[Ca^{2+}]_m$ in the mitochondrial matrix at sufficient level over long term. Here, we demonstrate that a sustained activity of eTRPM8 in HEK and HaCaT cells results in oscillatory Ca^{2+} releases from the ER of (Fig. 3A) which were associated with an oscillatory $[Ca^{2+}]_m$ changes (Fig. 3B) reflecting repetitive Ca^{2+} re-uptake into the

Figure 1. (see previous page) Modalities of eTRPM8 channel activation definite opposite response of cell growth. (A). Schematic representation of the structure of a monomeric eTRPM8 protein in the ER membrane. (B). Bar diagram plot illustrates growth (see Methods) of HaCaT keratinocyte cell line during 3 d. Cells were incubated at different temperature (37°C, 31°C, 25°C) or in presence of, daily-renewed, 10 μM icilin (Icilin). Alternatively, Icilin was applied for 10 minutes, and then washed out for 50 minutes; 8 cycles were achieved per day during 3 d (Pulsed Icilin). Data are presented as fold increase of the cell number from day 0 and have been normalized by the control condition (37°C). n = 3. §: $p < 0.05$. (C). As (B) in control HaCaT cells (CTL) or eTRPM8 knocked-down HaCaT cells incubated with or without pulsed stimulation with 20 μM icilin. n = ???, §: $p < 0.05$. (D). Dynamic of eTRPM8 transcription as measured by qPCR in HaCaT cell line incubated at different temperature or in presence of sustained icilin (20 μM) treatment. Values express Mean ± SD. n = 3. §: $p < 0.05$. (E). Radar plot summarizes normalized growth of control HaCaT cells (CTL), eTRPM8-overexpressing HaCaT cells (eTRPM8) and eTRPM8 knocked-down HaCaT cells (shM8) incubated in the same conditions as described in A. Value: mean. n = 3. (F). Bar diagram plot compares cell cycle analysis of control HaCaT cells (CTL) and eTRPM8 knocked-down HaCaT cells (shM8) with (white bars) or without (black bars) sustained treatment with 10 μM Icilin. Values express Mean ± SD. n = 3. a: $p < 0.05$ between CTL and shM8; b: $p < 0.05$ between control and icilin treatment.

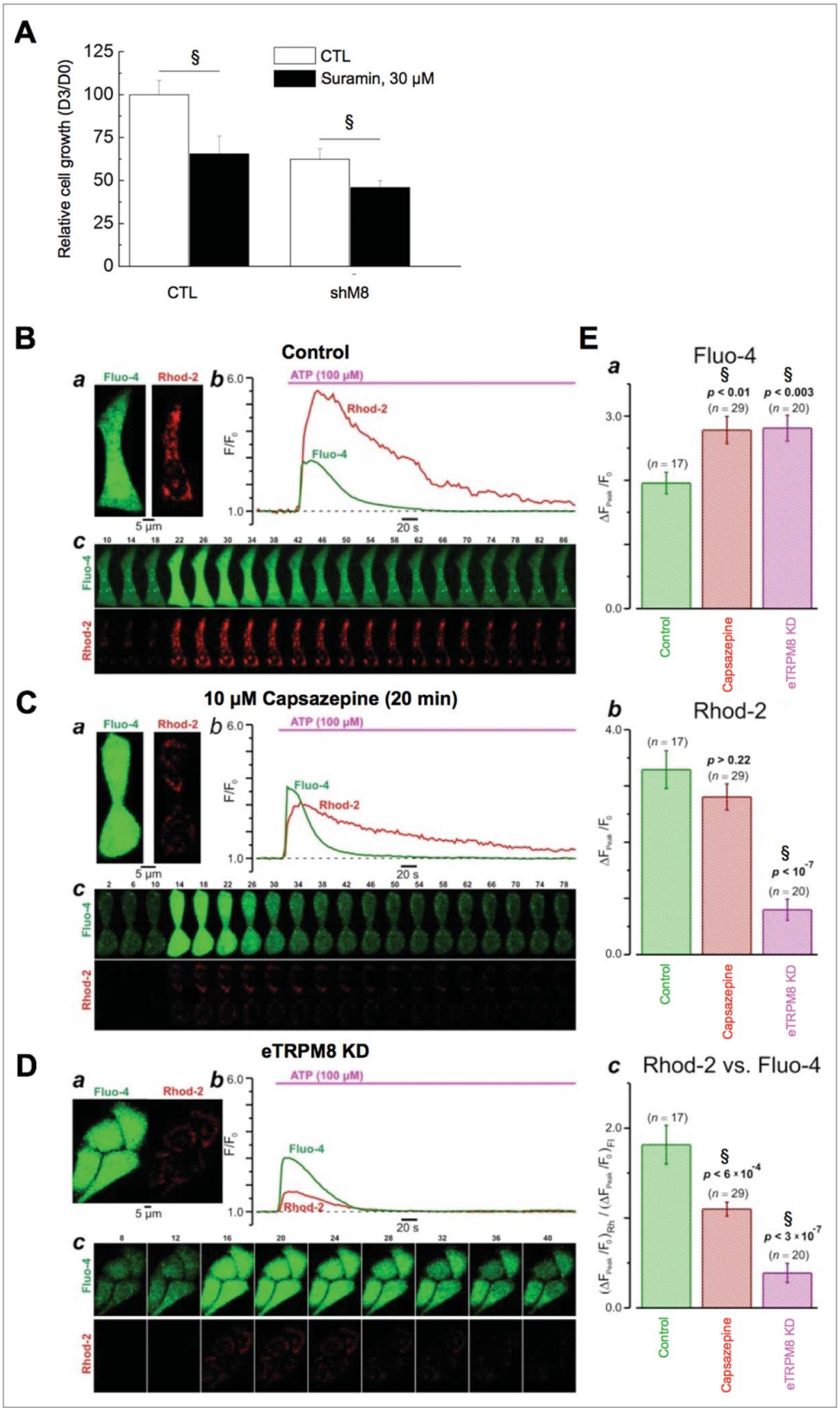

Figure 2. (For figure legend, see page 325.)

mitochondria over the period of at least 30 minutes. These oscillations were inhibited by capsazepine (Fig. 3B; insets) and were never observed in HaCaT cells with mutated pore region of eTRPM8.[8] Similar cytosolic and mitochondrial Ca^{2+} oscillations and their role in the regulation of hepatocyte metabolism have been reported previously. [13,14] Maintenance of this oscillatory Ca^{2+} transfer requires (1) refilling of the ER with Ca^{2+} and (2) a repetitive Ca^{2+} extrusion from mitochondria, which may serve to prevent activation of cyclophilin D and the permeability transition **pore** in mitochondria (for a review see ref. [15]). By means of FRET-FLIM of D1ER and mtD3CPV biosensors expressed in the ER and mitochondria of HaCaT cells, respectively, we measured steady-state $[Ca^{2+}]$. We found that incubation of HaCaT at 31°C did not alter $[Ca^{2+}]_{ER}$ (Fig. 3C) but significantly decreased $[Ca^{2+}]_m$ (Fig. 3D). It should be noted that the overexpression of eTRPM8 partially attenuated the $[Ca^{2+}]_m$ decrease at 31°C while but not at 25°C (Fig. 3E). This is along the line of our previous observation of correlation between eTRPM8-mediated $[Ca^{2+}]_m$ elevation and an increased bioavailability of ATP at 31°C.[8] At 25°C, however, both $[Ca^{2+}]_{ER}$ and $[Ca^{2+}]_m$ are significantly reduced (Fig. 3C and D). This may reflect a reduction in the efficiency of the Ca^{2+} re-uptake into the ER, which, in turn, will lead to a decrease of the Ca^{2+} release from the ER and, hence, to attenuation of the mitochondrial Ca^{2+} uptake, so that Ca^{2+} extrusion from mitochondria will eventually prevail. Even though eTRPM8 mRNA level is increased after a 3-day incubation at 25°C (Fig. 1B), concurrent decrease of the ER Ca^{2+} load overrides the effect of the eTRPM8 upregulation and $[Ca^{2+}]_m$ continue to decline.

Summing up, at skin average temperature (range 31–33°C), eTRPM8 mediates Ca^{2+} oscillations in the mitochondrial matrix, thus preventing drop of ATP production. At colder temperatures, the sustained eTRPM8 activity contributes to the ER Ca^{2+} leak that overrides Ca^{2+} uptake into the ER mediated by SERCA, the activity of which is reduced due to the dramatic drop in [ATP]. This leads to a decrease in ER Ca^{2+} content what creates an adverse cycle inducing a drop in $[Ca^{2+}]_m$, an increase in $[O_2^{\bullet-}]$ [8] and further decrease in [ATP].[8] Such a decrease in the ER Ca^{2+} content mimics the effects of eTRPM8 inhibition/suppression and may explain why sustained activation of eTRPM8 by cold leads to biological outcomes (e.g., decrease in cell growth) similar to those cased by its suppression.

Acute cold induces an eTRPM8-dependent and ROS-mediated necrosis of keratinocytes

One striking feature of keratinocytes incubated at 25°C is dramatic decrease of $[Ca^{2+}]_m$, $[Ca^{2+}]_{ER}$ and [ATP], and attenuation of cellular processes: proliferation, late differentiation markers.[8] General suppresion of cell function with concurrent increase in oxidative stress (observed elevation of $O_2^{\bullet-}$) is a good predictive marker for necrosis. This prompts us to assess necrosis in the keratinocytes incubated for 3 d at 25°C. As it is depicted by dark blue-stained cells on the images (Fig. 4) and is quantified in bar diagram plot (Fig. 5A), the fraction of necrotic cells was negligibly small in control cells incubated at 37°C and 31°C but was elevated to 12% following 3-day incubation at 25°C. Overexpression of eTRPM8 sensitizes the cells to necrosis at 31°C and dramatically augments necrosis at 25°C (35%). Interestingly, an augmentation of necrosis by eTRPM8 overexpression can be virtually completely reversed by the concomitant overexpression of the superoxide dismutase 1 (SOD1). This suggested a causal link between $[O_2^{\bullet-}]$ and necrosis, which was confirmed further by correlation analysis (Fig. 5B).

In conclusion, in our recent study and in this addendum, we characterized a new isoform of the icilin-activated cold receptor TRPM8 channel, eTRPM8,

Figure 2. (see previous page) Interplay between eTRPM8 and the purinergic pathway controls the proliferation of keratinocytes at 37°C. (A). Bar diagram plot illustrates growth of HaCaT keratinocyte cell line during 3 d. Cells were incubated with or without 30 μM Suramin in order to inhibit purinergic receptors. Data are presented as fold increase of the cell number from day 0 and have been normalized by the control condition. n = 3. §: $p < 0.05$. (B). Effect of eTRPM8 inhibition on cytosolic (fluo-4) and mitochondrial (rhod-2) $[Ca^{2+}]$ transients induced by 100 μM ATP in HaCaT cells. The plots (b) show the time course of ATP-induced changes in the fluorescence intensity (F/F_0) of fluo-4 and rhod-2 (as indicated) for the cell(s) in control (a, top) and following 20 min incubation with 10 μM capsazepine (C). The galleries (c) show confocal images of fluo-4 and rhod-2 fluorescence captured at times depicted above the images. (D). The same as B but obtained from eTRPM8 knockdown HaCaT cells. Note, that plots in (Cb, bottom) and in (Db) show mean traces for the 2 and 4 cells, respectively. E. The bar diagram plots compares the peak amplitudes of the ATP-induced responses ($\Delta F/F_0$) in cytosol (a), mitochondria (b) and the peak amplitudes of mitochondrial response normalized to that in cytosol (c). The number of responses analyzed (*n*) and *p* are indicated above the bars.

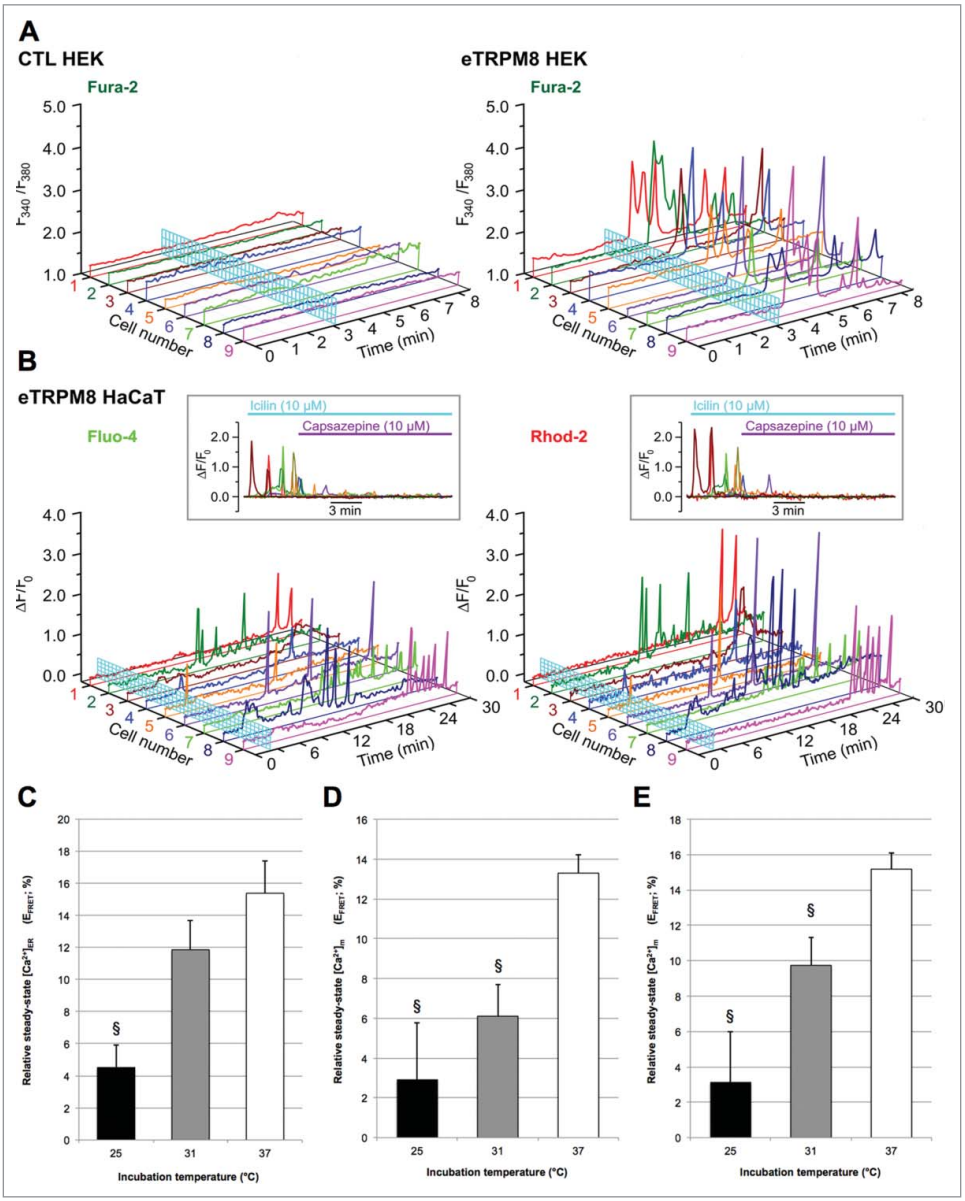

Figure 3. eTRPM8 mediates a sustained and oscillatory Ca^{2+} shuttling from the ER to mitochondria. (A). Changes of Ca^{2+} concentration in cytosol ($[Ca^{2+}]_c$) in response to external application of 10 μM icilin were monitored using *x-y* time series imaging of fura-2 in control vs. eTRPM8-overexpressing HEK cell line. (B). Concomitant monitoring of relative changes of Ca^{2+} concentration ($\Delta F/F_0$) in cytosol ($[Ca^{2+}]_c$) and mitochondria ($[Ca^{2+}]_m$) in response to external application of 10 μM icilin was performed in eTRPM8-overexpressing HaCaT cells using fluo-4 and rhod-2 fluorescence, respectively. Insets: Inhibition of the incilin-induced oscillations of $[Ca^{2+}]_c$ and $[Ca^{2+}]_m$ with 10 μM icilin capsazepine (n = 8). (C). Bar diagram plot shows the apparent steady-state Ca^{2+} concentration in ER ($[Ca^{2+}]_{ER}$) in control HaCaT cells as measured by FRET-FLIM of D1ER biosensor (see Methods). Apparent steady-state $[Ca^{2+}]_m$ has been measured in both control HaCaT cells. (D). or in eTRPM8-overexpressing HaCaT cells. (E). Values express Mean ± SD. n = 15 cells per conditions. §: $p < 0.05$.

whose 4 transmembrane domains-based structure and localization in the ER microdomaines confer its unique role as cold transducer regulating mitochondrial bioenergetics in keratinocytes. We demonstrated that the level of expression of eTRPM8 and the modalities of its activation by cold determine the [ATP] / $[O_2^{\bullet-}]$ ratio via fine tuning of $[Ca^{2+}]_m$ and $[Ca^{2+}]_{ER}$. This consequently determines the keratinocyte fate (Fig. 5C).

Materials and methods

Cell culture

HaCaT cell line was grown in Dulbecco's minimal essential media (DMEM) (Gibco) supplemented with

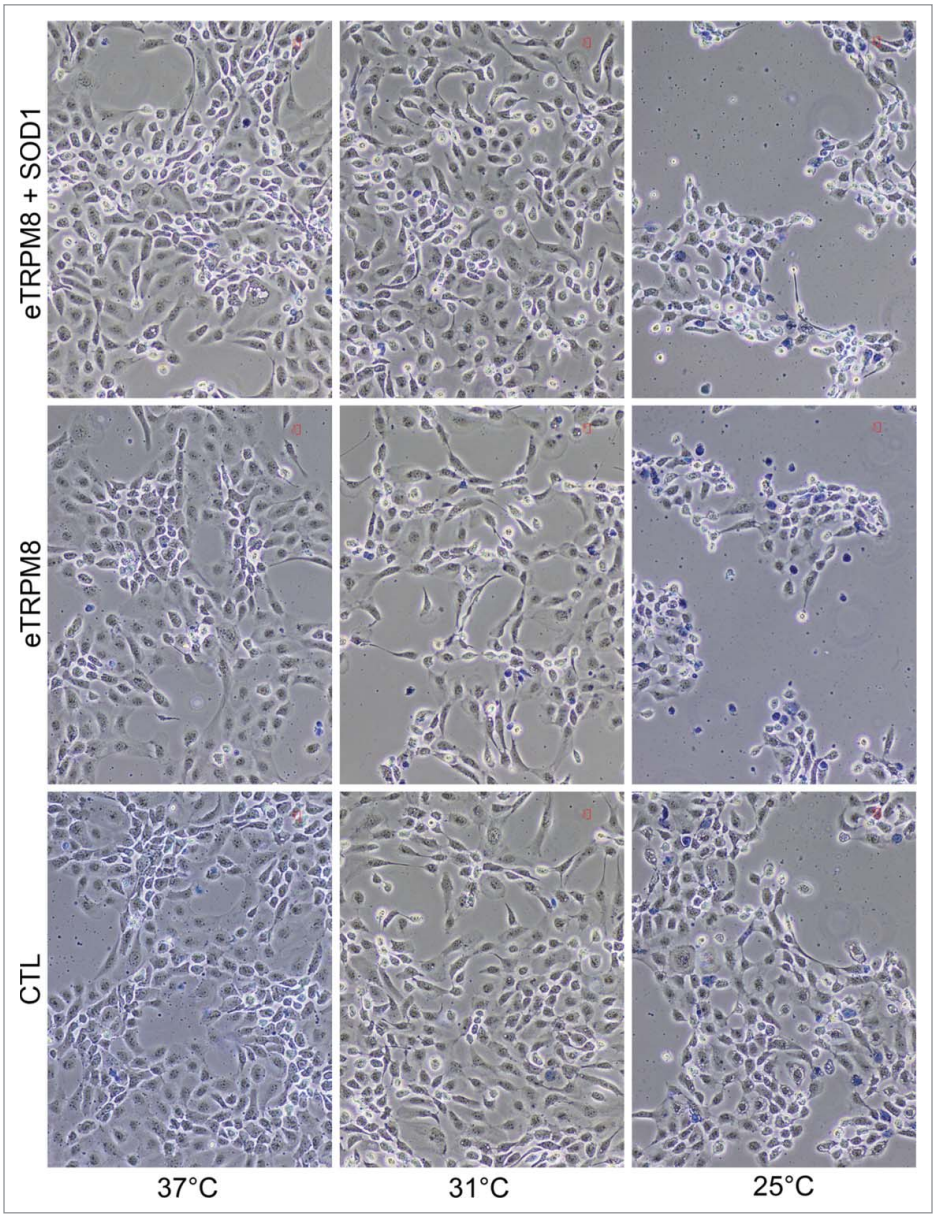

Figure 4. A sustained cold-mediated TRPM8 activity induces necrosis of keratinoyctes. Images shows a Trypan blue staining of control HaCaT cells (CTL), eTRPM8-overexpressing HaCaT cells (eTRPM8) or HaCaT cells concomitantly overexpressing eTRPM8 and the superoxide dismutase 1, SOD1 (eTRPM8+SOD1) incubated at 37°C, 31°C or 25°C for 3 d. Necrotic cells appeared as dark blue-stained cells.

2% fetal calf serum (FCS) and Kanamycin (100 μg/ml), and [Ca^{2+}] was adjusted to 1.8 mM to induce differentiation, as described previously.[9] Necrosis was assessed by the mean of Trypan Blue.

Transient expression studies

Plasmid transfection was carried out with X-tremeGENE HP DNA Transfection Reagent (Roche) at the concentration of 4 μg per million cells. SiRNA transfection was performed with 50 nM of HiPerfect transfection reagent (Qiagen).

siRNA and shRNA plasmids were built in pENTER vector (Invitrogen) following manufacturer's recommendations. Control shRNA targeted TRPM8 exon 7 and shRNA anti-eTRPM8 targeted exon 20. shRNA sense sequences are: CACCAtctctgagcgcactattcaGAGAGtgaatagtgcgctcagaga and CACCAtattccgttcggtcatctaGAGAGtagatgaccgaacggaata (Capital letters refer to the structure of the short hairpin RNA and small letters

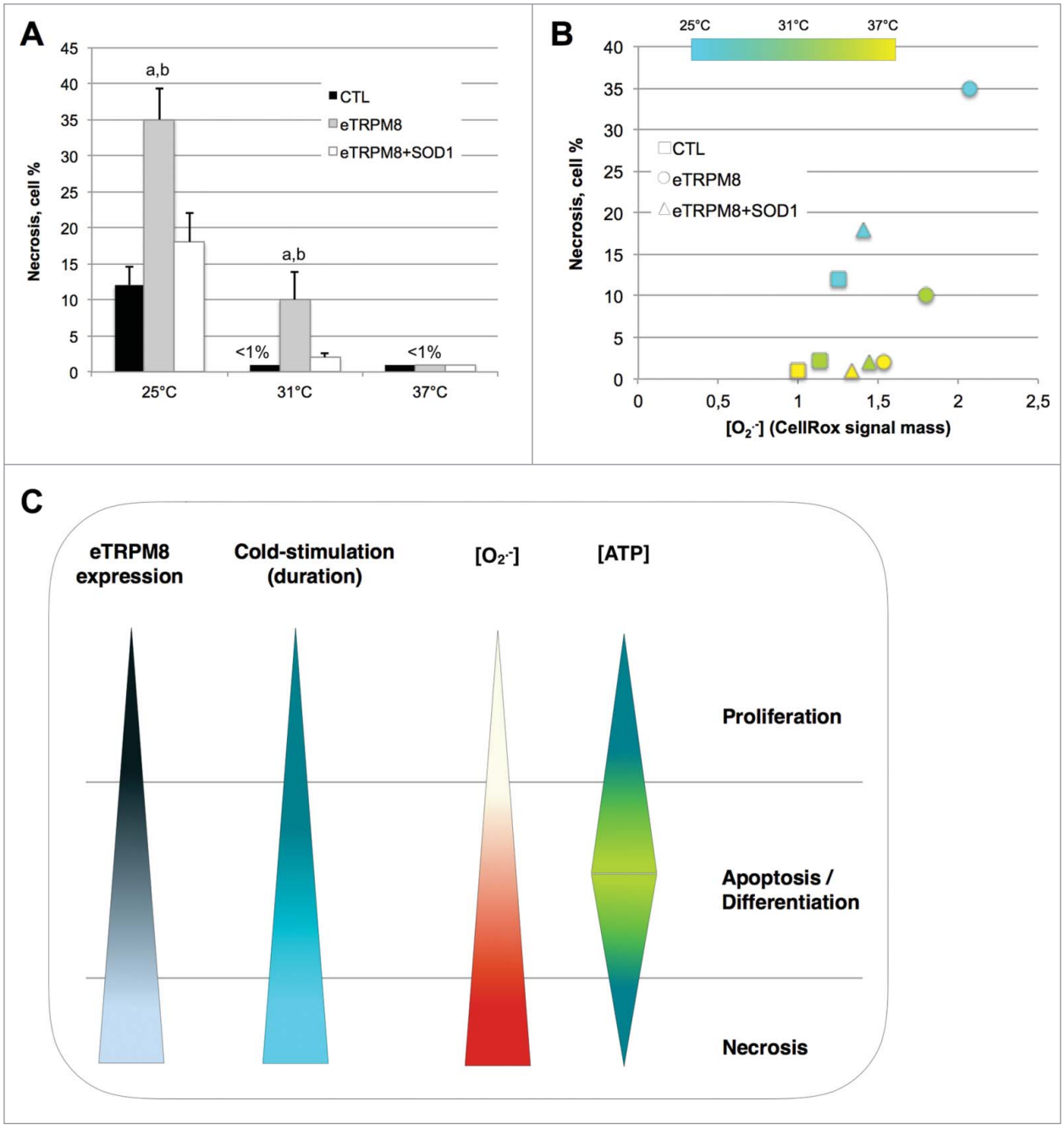

Figure 5. Cold, below 25°C, induces an adverse cycle leading to ROS-mediated necrosis of keratinocytes. (A). Bar diagram plot represents the proportion of necrosis in the HaCaT cell population as quantified by counting of images presented in the Fig. 4. Values express Mean ± SD. n = 3. a: $p < 0.05$ between CTL cells and eTRPM8-overexpressing cells (eTRPM8); b: $p < 0.05$ between eTRPM8 cells and cells concomitantly overexpressing eTRPM8 and the superoxide dismutase 1, SOD1 (eTRPM8+SOD1). (B). Scatter plot demonstrates the correlation between superoxide concentration ($[O_{2.}^{-}]$) in mitochondria (see Methods) and the proportion of necrosis in the HaCaT cell population. Control cells were compared to cells overexpressing either eTRPM8 or eTRPM8+SOD1 and were incubated at different temperature for 3 d. Values express Mean of 3 independent experiences. (C). Scheme illustrating the correlation between eTRPM8 expression level, the modalities (intensity, duration, frequency) of the cold stimulation, $[O_{2.}^{-}]$ and [ATP], and cell fate (Proliferation, Apoptosis/differentiation, necrosis).

refer to the siRNA sequence). Control of silencing efficiency was achieved by immunoblotting of total proteins extracted from Hek cells, co-transfected with either shCTL + eTRPM8pcDNA4 or shM8 + eTRPM8pcDNA4.

Control siRNA targeted Luciferase (siCTL) and siRNA anti-eTRPM8 (siTRPM8) targeted exon 20. The sense sequences are CUUACGCUGAGUACUUCGA(dTdT) and GUAUUCUGGACGAGUCAUU(dTdT), respectively.

Analysis of TRPM8 mRNA expression

Total RNA was isolated from different cell lines using Tri Reagent mix (Sigma-Aldrich). After a DNase I (Invitrogen) treatment and phenol/chloroform purification, 2 μg of total RNA was reverse transcribed into cDNA at 42°C using random hexamer primers (Applera) and MuLV reverse transcriptase (Applera).

Qualitative PCR was performed with TaqGold polymerase (Applera) and controlled on agarose gel.

Real-time quantitative PCR was performed on a Cfx C1000 system (Biorad). For each reaction, 12.5 ng of cDNA was placed in 15 μl of final reaction medium containing 7.5 μl of 2x SsoFast™ EvaGreen® Supermix (Biorad) and 200 nM primer pairs: CGGTCATCTACGAGCCCTAC and CACACACAGTGGCTTGGACT. The housekeeping gene Glyceraldehyde-3-phosphate dehydrogenase (GAPDH) was used as an endogenous control to normalize variations in RNA extracts, the degree of RNA degradation and variability in RT efficiency. GAPDH prmiers were: ACCCACTCCTCCACCTTTG and CTCTTGTGCTCTTGCTGGG. To quantify the results, we used the comparative Ct method. PCR protocol consisted of: 30 s denaturation at 95°C followed by 40 cycles of [4 s at 95°C and 30 s at 60°C], and final dissociation curve to control specificity of the amplification.

Flow cytometry was conducted with CyAn™ ADP Analyzer. Cells were harvested, then suspended in 250 μl PBS / 4% BSA / 0,1% Triton X100 with Ribonuclease A (200 μg/ml) and incubated at room temperature for 15 min. After addition of 250 μl of PBS containing 30 μg/ml of propidium iodide, cells were further incubated at room temperature for 30 min to 1 hour. Data were analyzed with FlowJo software (version 8.7).

Visualization of agonist-induced changes of Ca^{2+} concentration in cytosol ($[Ca^{2+}]_c$) and mitochondria ($[Ca^{2+}]_m$)

Changes of $[Ca^{2+}]_c$ were imaged using the high-affinity fluorescent Ca^{2+} indicator fluo-4, as described previously.[16,17] Fluo-4 was loaded by 1-hour incubation of the cells with 5 μM fluo-4 acetoxymethyl ester (fluo-4 AM; diluted from a stock containing 2 mM fluo-4 AM and 0.025% (w/v) pluronic F-127 in dimethyl sulphoxide). Changes of $[Ca^{2+}]_m$ were imaged using fluorescent Ca^{2+} indicator rhod-2: 50 μg of rhod-2 AM was dissolved in 10 μl of DMSO (containing 0.025% (w/v) pluronic F-127), which was then mixed with 4 ml of PSS and superfused to the experimental chamber for 20 min. The incubation of the cells with the dyes was followed by a 1-hour wash in PSS containing 1.7 mM $CaCl_2$ to allow time for de-esterification. The dye loading was performed at RT. The cells were then kept for 30 min at 37°C. Before imaging was commenced the cells were superfused with PSS containing 70 μM $CaCl_2$ and supplemented with 10 μM $LaCl_3$ to eliminate capacitative Ca^{2+} entry, unless stated otherwise. The cells were stimulated with 10 μM icilin. The intensity of fluo-4 or rhod-2 fluorescence (F) was normalized to the average fluorescence intensity in the images acquired before agonist application (F_0). The temporal profiles of the agonist-induced $[Ca^{2+}]_c$ and $[Ca^{2+}]_m$ transients are illustrated by the plots showing time course of the normalized fluo-4 or rhod-2 fluorescence intensity (F/F_0) averaged within confocal optical slice of the cell.

Superoxide assessment

HaCaT cells were transfected with empty vector (CTL), eTRPM8 plasmid or eTRPM8 + SOD1 plasmids. Cells were incubated in the medium supplemented with 2.5 μM CellRox® Deep Red reagent for 30 min at 37°C. After two washes, cells were incubated for 30 min at 37°C prior to confocal imaging. For each temperature and siRNA condition, the measurements were performed in 3 Petri dishes, sequentially mounted on the microscope stage at the ambient temperature corresponding to the pre-incubation temperature. In each Petri dish, confocal imaging of CellRox® Deep Red fluorescence was performed from 4 regions of interest, 230 × 230 μm (1024 × 1023 pixels) each. The same illumination intensity, photomultiplier gain and offset were used in all the experiments. Data were processed with ImageJ64 freeware. After setting offset (pixel fluorescence intensity below 20 a.u.) and the mean cell background (pixel fluorescence intensity 100 a.u.) in the control condition (cells grown at 37°C), specific to $O_2^{\bullet-}$ increase in the CellRox® Deep Red fluorescence was computed according to the formula $\sum Pix_{I(100-255)} / \sum Pix_{I(20-255)}$, where $Pix_{I(20-255)}$ and $Pix_{I(100-255)}$ are the pixels with intensities lying within the range of 20–255 and 100–255 a.u.,

respectively. The $O_2^{\bullet-}$- specific increases in the CellRox® Deep Red signal mass for each condition were averaged, normalized to the mean value, detected at 37°C either in HaCaT cells. Data are presented in the Figure 5B as mean.

Confocal microscopy

Experimental chambers with the cells were placed on the stage of Axiovert 200M inverted microscope attached to a LSM 510 META laser-scanning unit (Zeiss, Oberkochen, Germany). The SCSi interface of the confocal microscopes was hosted by a Pentium PC (32-bit Windows NT 4.0 operating system) running LSM 510 software (Zeiss, Oberkochen, Germany). During time series protocol, the x-y confocal images of the fluo-4, rhod-2 fluorescence were acquired at 0.1–0.5 Hz using a Zeiss plan-Apochromat 40× 1.3 N. A. or 63× 1.4 N.A. oil-immersion objectives. Fluo-4 fluorescence was excited by the 488 nm line of a 500 mW argon ion laser (Laser-Fertigung, Hamburg, Germany) and was captured at wavelengths 505-530 nm. Rhod-2 fluorescence was exited by the 543 nm line of 15 mW helium/neon ion laser and detected at wavelengths 560–615 nm. The illumination intensity was attenuated to 0.5–6 % (depending on the laser line) with an acousto-optical tunable filter (Zeiss, Oberkochen, Germany). To optimize signal quality the pinhole was set to provide a confocal optical section 0.5–1.8 μm, depending on experimental protocol. To avoid any bleed-through of the fluorescence signal in multi-staining experiments, fluorochromes with well separated excitation and emission spectra were used and imaging was performed using the frame-by-frame multitrack mode of the confocal scanner: sequential acquisition via well-separated optical channels of the x-y images produced by fluorescence of different fluorochromes. The photomultiplier gain and offset in each optical channel were set individually to achieve similar signal intensity at each channel and remove sub-signal noise from the images. The adequacy of the imaging protocol applied to the multi-labeled myocytes was confirmed by control experiments on the mono-labeled cells.

Experimental solutions

In confocal microscopy experiments the cells were bathed in physiological salt solution (PSS) containing (in mM): NaCl 140, KCl 5, $MgCl_2$ 1, glucose 10, HEPES 10; pH adjusted to 7.4 with NaOH. PSS was supplemented with 70 μM or 1.7 mM $CaCl_2$, depending on experimental protocol, as described in the text.

Data analysis and statistical procedures

Each experiment was repeated at least 3 times independently. Data are expressed as mean ± S.D when not indicated in legends. The data were analyzed and graphs plotted using Origin 5.0 software (Microcal, Northampton, MA, USA). InStat3 (GraphPad Software Inc., SanDiego, USA) was used for statistical analysis and the mean values were compared using either unpaired *t*-test with Welch's corrected test (2 groups) or One-way ANOVA with Dunnett multiple comparison post-test (≥3 groups). Statistical significances were: § $p < 0.05$.

Disclosure of potential conflicts of interest

No potential conflicts of interest were disclosed.

Acknowledgments

Authors thank Prof. Julien J-P. at the center de recherche CHU Laval, QUEBEC, for his generous gift of pcDNA3-FlagN-SOD1 plasmid.

Funding

This work has been supported by grants from: INSERM, Ministère de l'Education Nationale, Ligue Nationale Contre le Cancer, Region Nord-Pas-de-Calais and ANR Grant: TRPM8/Reprod. The Cosmetics department of Johnson & Johnson laboratories supported Dr. Gabriel Bidaux. Dr. Anne-sophie Borowiec was supported by Fondation pour la recherche médicale. Dr. Dmitri Gordienko was supported by State Found for Fundamental Research (F 46.2/001).

References

[1] Lumpkin EA, Caterina MJ. Mechanisms of sensory transduction in the skin. Nature 2007; 445:858-65; PMID:17314972; http://dx.doi.org/10.1038/nature05662

[2] Mandadi S, Sokabe T, Shibasaki K, Katanosaka K, Mizuno A, Moqrich A, Patapoutian A, Fukumi-Tominaga T, Mizumura K, Tominaga M. TRPV3 in keratinocytes transmits temperature information to sensory neurons via ATP. Pflugers Arch 2009; 458:1093-102; PMID:19669158; http://dx.doi.org/10.1007/s00424-009-0703-x

[3] Moqrich A, Hwang SW, Earley TJ, Petrus MJ, Murray AN, Spencer KS, Andahazy M, Story GM, Patapoutian A. Impaired thermosensation in mice lacking TRPV3, a heat and camphor sensor in the skin. Science 2005;

307:1468-72; PMID:15746429; http://dx.doi.org/10.1126/science.1108609

[4] Dhaka A, Viswanath V, Patapoutian A. Trp ion channels and temperature sensation. Annu Rev Neurosci 2006; 29:135-61; PMID:16776582; http://dx.doi.org/10.1146/annurev.neuro.29.051605.112958

[5] Smith AD, Crabtree DR, Bilzon JL, Walsh NP. The validity of wireless iButtons and thermistors for human skin temperature measurement. Physiol Meas 2010; 31:95-114; PMID:19940348; http://dx.doi.org/10.1088/0967-3334/31/1/007

[6] McKemy DD, Neuhausser WM, Julius D. Identification of a cold receptor reveals a general role for TRP channels in thermosensation. Nature 2002; 416:52-8; PMID:11882888; http://dx.doi.org/10.1038/nature719

[7] Peier AM, Moqrich A, Hergarden AC, Reeve AJ, Andersson DA, Story GM, Earley TJ, Dragoni I, McIntyre P, Bevan S, et al. A TRP channel that senses cold stimuli and menthol. Cell 2002; 108:705-15; PMID:11893340; http://dx.doi.org/10.1016/S0092-8674(02)00652-9

[8] Bidaux G, Borowiec AS, Gordienko D, Beck B, Shapovalov GG, Lemonnier L, Flourakis M, Vandenberghe M, Slomianny C, Dewailly E, et al. Epidermal TRPM8 channel isoform controls the balance between keratinocyte proliferation and differentiation in a cold-dependent manner. Proc Natl Acad Sci U S A 2015; 112:E3345-54; PMID:26080404; http://dx.doi.org/10.1073/pnas.1423357112

[9] Borowiec AS, Delcourt P, Dewailly E, Bidaux G. Optimal differentiation of in vitro keratinocytes requires multifactorial external control. PLoS One 2013; 8:e77507; PMID:24116231; http://dx.doi.org/10.1371/journal.pone.0077507

[10] Rohacs T, Lopes CM, Michailidis I, Logothetis DE. PI(4,5)P2 regulates the activation and desensitization of TRPM8 channels through the TRP domain. Nat Neurosci 2005; 8:626-34; PMID:15852009; http://dx.doi.org/10.1038/nn1451

[11] Lee WK, Choi SW, Lee HR, Lee EJ, Lee KH, Kim HO. Purinoceptor-mediated calcium mobilization and proliferation in HaCaT keratinocytes. J Dermatol Sci 2001; 25:97-105; PMID:11164706; http://dx.doi.org/10.1016/S0923-1811(00)00117-1

[12] Greig AV, Linge C, Cambrey A, Burnstock G. Purinergic receptors are part of a signaling system for keratinocyte proliferation, differentiation, and apoptosis in human fetal epidermis. J Invest Dermatol 2003; 121:1145-9; PMID:14708618; http://dx.doi.org/10.1046/j.1523-1747.2003.12567.x

[13] Robb-Gaspers LD, Burnett P, Rutter GA, Denton RM, Rizzuto R, Thomas AP. Integrating cytosolic calcium signals into mitochondrial metabolic responses. EMBO J 1998; 17:4987-5000; PMID:9724635; http://dx.doi.org/10.1093/emboj/17.17.4987

[14] Robb-Gaspers LD, Rutter GA, Burnett P, Hajnoczky G, Denton RM, Thomas AP. Coupling between cytosolic and mitochondrial calcium oscillations: role in the regulation of hepatic metabolism. Biochim Biophys Acta 1998; 1366:17-32; PMID:9714714; http://dx.doi.org/10.1016/S0005-2728(98)00118-2

[15] Rasola A, Bernardi P. Mitochondrial permeability transition in Ca(2+)-dependent apoptosis and necrosis. Cell Calcium 2011; 50:222-33; PMID:21601280; http://dx.doi.org/10.1016/j.ceca.2011.04.007

[16] Povstyan OV, Harhun MI, Gordienko DV. Ca2+ entry following P2X receptor activation induces IP3 receptor-mediated Ca2+ release in myocytes from small renal arteries. Br J Pharmacol 2011; 162:1618-38; PMID:21175582; http://dx.doi.org/10.1111/j.1476-5381.2010.01169.x

[17] Thebault S, Lemonnier L, Bidaux G, Flourakis M, Bavencoffe A, Gordienko D, Roudbaraki M, Delcourt P, Panchin Y, Shuba Y, et al. Novel role of cold/menthol-sensitive transient receptor potential melastatine family member 8 (TRPM8) in the activation of store-operated channels in LNCaP human prostate cancer epithelial cells. J Biol Chem 2005; 280:39423-35; PMID:16174775; http://dx.doi.org/10.1074/jbc.M503544200